

Simulation of Nonuniform High-speed Interconnects with Frequency Dependent Parameters by Wavelets on the Interval

S. Barmada, M. Raugi

Dipartimento di Sistemi Elettrici e Automazione,
Università di Pisa, via Diotisalvi, 2 56126 Pisa Italy
Tel: +39 050 565111 Fax: +39 050 565333
sami.barmada@dsea.unipi.it raugi@dsea.unipi.it

Abstract

A wavelet approach to the analysis of nonuniform high-speed interconnects with frequency dependent parameters is presented in this paper. The nonuniform interconnects are modeled by the use of nonuniform multiconductor transmission line equations in the frequency domain. Two different methods are proposed here (differential and integral formulation): in both of them the space variable is expanded on a wavelet basis, yielding an algebraic system in the wavelet - frequency domain. The algebraic system is then easily solved by the use of standard techniques; the results are inverse transformed yielding the behavior of voltage and current in the frequency domain. Inverse FFT (Fast Fourier Transform) gives the time domain solution.

1 Introduction

The transient analysis of interconnections is a fundamental tool for the synthesis and design of high speed systems such as printed circuit board (PCB) or multichip modules (MCM) in order to determine distortion, crosstalk and other EMC effects that can affect the performances of high density electronics.

A number of numerical techniques [1]-[10] have been reported in the past for the computer simulation of these systems, initially considering uniform lines, and subsequently taking into account nonuniformity and frequency dependent parameters, whose effects cannot be actually neglected in high speed applications.

The Fourier or Laplace transform techniques usually require the inversion of transcendental or hyperbolic functions and in many cases are not efficient; the method of characteristics has been coupled with recursive convolution integral or line discretization along the length and was generalized for skin-effect problems at the cost of an increase of CPU times or memory requirements, furthermore in some cases an accurate evaluation of the impulse response of the line is required. The waveform relaxation is an iterative technique that solves the TL equations in the frequency domain and uses FFT to transform the results back and forth between time and frequency domain at each iteration, but would require too many data points to avoid aliasing effects when very fast signals have to be studied.

Numerical modeling directly in the time domain by differential methods (DM), mainly based on finite elements (FE) and finite-difference time-domain (FDTD), yields a straight modeling of the problem but it is normally coupled with convolution integrals. Furthermore, these methods need dense discretization of the line where the signal is rapidly varying, since the signal propagates along the line the discretization in space should "follow" the signal motion, and this usually leads to the adoption of very fine discretization both in time and space yielding remarkable CPU times.

The wavelet expansion of a function in space characterizes the "harmonic" content of the function at every coordinate, then wavelet basis functions have very good localization properties in space. In particular

the ability of wavelets to focus on short interval for high frequency components and long intervals for low frequency components makes the method effective to represent non-smooth functions since they automatically concentrate in the fast varying regions, and therefore overcoming the DM limitations.

Recently wavelet expansion has been used to solve TL transients [11]. Voltages and currents have been expanded in space by wavelets and a representation of the entire line has been obtained. The final equation is a function of time that is numerically integrated with a standard Runge-Kutta method.

Wavelet expansion has already been used by the authors for the solution of MTL transients [12], [13]; in this paper frequency dependent parameters coupled with nonuniformity have been included. Non-linearities are not included here, but the problem here studied is anyway challenging since there are several applications in which linear loads and frequency dependent parameters are present. Wavelet expansion in space is applied to frequency domain MTL nonuniform equations yielding an algebraic system whose solution, represented by the sample of voltages at the line ports in the frequency domain, is transformed in time domain by FFT. Hence, a numerical solution with no time stepping and iterative procedures has been developed avoiding also the inversion of transcendental functions is obtained. Besides by the use of the WE the system matrices are highly sparse, and by the use of numerical techniques optimized for sparse matrices, very low CPU times can be obtained. Furthermore by thresholding the elements of the matrix [16] it is possible control the sparsity of the system, hence to control the CPU time, while the accuracy of the results are not dramatically affected. This discretization procedure produces systems of algebraic equations which have good condition numbers.

Among the many available wavelet basis in the literature, we choose the compact support Daubechies wavelets and wavelets on the interval. They have the advantage of correctly representing polynomials of degree N and their regularity increases with N (N number of their vanishing moments), more exactly the Holder continuity coefficient increases with N . A greater regularity leads also to a wider numerical support, then there is a trade-off between the order of the approximation and the numerical cost.

2 Wavelets on the Interval and Operators

The concepts of scaling functions, wavelets, time-scale analysis, multiresolution analysis are here considered known [14]; there are many wavelets basis available in the literature, and we chose the Daubechies Wavelets on the interval [15] for their numerical properties. In particular the choice of wavelets that "survive" only on intervals is adopted because we are interested in the solution of boundary value problems. For the compact support wavelet there is an important relation that allows a straight computation of the wavelet coefficients of a generic function: it is possible to obtain the coefficients from the samples of the functions itself according to the relation $\langle \phi_{J,k}, f \rangle = 2^{J/2} f(2^J k)$, where $\phi_{J,k}$ is the scaling function of order J, k of the adopted wavelet basis. Then, the vector of wavelet coefficients $G = \mathbf{W}g(t_j)$ representing the wavelet transform of a function $g(t)$ can be obtained by multiplying a matrix \mathbf{W} related to the adopted wavelet basis and the time samples $g(t_j)$ corresponding to 2^{-m} equally spaced points in the interval $[0, 1]$. Further details about wavelet numerical computation can be found in [16].

The Wavelet Expansion is used to transform a signal into a vector of coefficients according to the relation

$$f(t) = \mathbf{b}(t)\mathbf{f} \quad (1)$$

where $\mathbf{b}(t)$ is the wavelet basis and \mathbf{f} is the vector of coefficients constituting the wavelet expansion of the signal. The notation described in (1) will be used throughout the paper.

Wavelets can also represent operators [17]; in particular an operator in the wavelet domain is represented by a matrix of constant entries. The entries of course depend on the chosen basis and the chosen resolution. A representation of the differential and integral operator for the Daubechies wavelets on the interval has been developed by the authors [12], [13]. The matrices obtained are sparse, as shown in the mentioned papers, and this is important for the numerical characteristic of the obtained method and for the CPU times. Besides in this paper we use also the multiplication by an operator in the wavelet domain, as obtained in [12] and [13]. This allows the representation of nonuniform lines in the wavelet domain when wavelet expansion in space is performed.

2.1 Solution of first order differential equations in the wavelet domain

The following is a differential equation and the relative boundary condition:

$$\dot{y} + ay = u \quad y(0) = y_0 \quad (2)$$

By expanding $y(t)$ and exploiting the definition of operators on a wavelet basis we obtain the system:

$$\begin{cases} \mathbf{D}\mathbf{Y} + a\mathbf{Y} = \mathbf{U} \\ \mathbf{b}_0\mathbf{Y} = y_0 \end{cases} \quad (3)$$

Vectors \mathbf{Y} and \mathbf{U} are vectors representing the wavelets coefficients of the unknowns y and the known terms u and their dimension is 2^{-m} (with $m < 0$), according to the chosen resolution. The subscript 0 denotes the lower bound value of \mathbf{Y} ; \mathbf{D} is the differential operator and has dimension $2^{-m} \times 2^{-m}$ and the differentiation is performed in the wavelet domain simply by multiplying the matrix by the vector of coefficients representing the quantity to be derived. \mathbf{b}_0 is a constant vector, whose components are the values of the basis functions on the left border of the interval. System (3) can be solved only in the least square sense since it is characterized by $n + 1$ equations in n unknown wavelet coefficients. Nevertheless the solution gives accurate result. Qualitatively this fact can be explained because the initial condition has to be known to solve the problem, then the first n equations cannot represent the actual solution.

Indeed, the matrix $\mathbf{D} + a\mathbf{I}$ is very ill conditioned, furthermore when $a = 0$ the differential operator \mathbf{D} cannot be inverted to obtain the solution because different functions have same derivatives, hence $\mathbf{D}^{-1}\mathbf{D} \neq \mathbf{I}$. This means that the information given by equation (2b) is necessary to determine the actual solution and does not yield a redundant boundary on the first n equation. To get the solution by a $n \times n$ system of equations the eq. (2b) has been included in the system modifying the operator \mathbf{D} and the known term as follows:

$$(\mathbf{D} + \mathbf{B}_0)\mathbf{Y} + a\mathbf{Y} = \mathbf{D}'\mathbf{Y} + a\mathbf{Y} = \mathbf{U} + \mathbf{Y}_0 \quad (4)$$

where \mathbf{B}_0 is a matrix with all rows equal to the \mathbf{b}_0 vector and \mathbf{Y}_0 is a vector with all elements equal to y_0 .

2.2 Solution of integral equations in the wavelet domain

The following is a general integral equation:

$$y(t) - y(0) + a \int_0^t y(\tau) d\tau = \int_0^t u(\tau) d\tau \quad (5)$$

and its representation in the wavelet domain is:

$$\mathbf{I}_d[\mathbf{Y} - \mathbf{Y}_0] + a\mathbf{T}\mathbf{Y} = \mathbf{T}\mathbf{U} \quad (6)$$

where \mathbf{I}_d is the identity matrix, \mathbf{T} is the wavelet representation of the integral operator and the capital letters denote vectors representing the wavelets coefficients of unknowns y and known terms u . The initial conditions are taken into account explicitly by the \mathbf{Y}_0 term. The \mathbf{Y} , \mathbf{Y}_0 , \mathbf{U} are again wavelet coefficients vectors, and their dimension is 2^{-m} (with $m < 0$), according to the chosen resolution. The matrix \mathbf{T} has dimension $2^{-m} \times 2^{-m}$ and the integration is performed in the wavelet domain simply by multiplying the matrix by the vector of coefficients representing the quantity to be integrated. The solution is easily obtained by the solution of an algebraic system and it is given by

$$\mathbf{Y} = (\mathbf{I}_d + a\mathbf{T})^{-1}(\mathbf{I}_d\mathbf{Y}_0 + \mathbf{T}\mathbf{U})$$

3 Mathematical Formulation

A single conductor nonuniform TL is characterized by the following equations in the frequency domain:

$$\begin{cases} \frac{\partial}{\partial z} \dot{V}(z) = -Z(z, \omega) \dot{I}(z) \\ \frac{\partial}{\partial z} \dot{I}(z) = -Y(z, \omega) \dot{V}(z) \end{cases} \quad (7)$$

where $Z(z, \omega)$ and $Y(z, \omega)$ are the per unit length impedance and inductance of the line.

In practical applications it is possible to separate the dependence of ω from the dependence from z (see [18], [19]) hence it is possible to write:

$$Z(z, \omega) = Z_1(z)Z_2(\omega) \quad Y(z, \omega) = Y_1(z)Y_2(\omega) \quad (8)$$

In the following subsections we will obtain the formulations both with the differential and with the integral operator.

3.1 Differential formulation

Let us define $\mathbf{b}(z) = [b_1(z), \dots, b_n(z)]$ as the wavelet basis in the space domain, we can write that

$$\dot{V}(z) = \mathbf{b}(z)\dot{\mathbf{V}} \quad \dot{I}(z) = \mathbf{b}(z)\dot{\mathbf{I}} \quad (9)$$

where $\dot{\mathbf{V}} = [\dot{V}_1, \dots, \dot{V}_n]^T$ and $\dot{\mathbf{I}} = [\dot{I}_1, \dots, \dot{I}_n]^T$ are vectors of phasors, i.e. the vectors of coefficients of the wavelet expansion.

Substituting the expansion (9) into (7) we obtain

$$\begin{cases} \frac{\partial}{\partial z} \mathbf{b}(z)\dot{\mathbf{V}} = -Z_2(\omega)\mathbf{b}(z)\mathbf{Z}_1\dot{\mathbf{I}} \\ \frac{\partial}{\partial z} \mathbf{b}(z)\dot{\mathbf{I}} = -Y_2(\omega)\mathbf{b}(z)\mathbf{Y}_1\dot{\mathbf{V}} \end{cases} \quad (10)$$

where \mathbf{Z}_1 and \mathbf{Y}_1 are respectively the matrices of $Z_1(z)$ and $Y_1(z)$ obtained as product between functions in the wavelet domain.

By left multiplying by $\mathbf{b}(z)^T$ and taking into account the definition of the differential operator in the wavelet domain we obtain that

$$\begin{cases} \mathbf{D}_z \dot{\mathbf{V}} = -Z_2(\omega)\mathbf{Z}_1\dot{\mathbf{I}} \\ \mathbf{D}_z \dot{\mathbf{I}} = -Y_2(\omega)\mathbf{Y}_1\dot{\mathbf{V}} \end{cases} \quad (11)$$

where \mathbf{D}_z is the matrix representing the differential operator in the wavelet domain.

The boundary conditions are given by the equations at the ports of the line; they are respectively

$$\begin{cases} \dot{V}(0) + Z_s \dot{I}(0) = \dot{E} \\ \dot{V}(L) = Z_L \dot{I}(L) \end{cases} \quad (12)$$

where Z_s , Z_L and \dot{E} are respectively the input and the output impedance, and the input generator phasor at a certain frequency.

In the wavelet domain we have

$$\begin{cases} \dot{V}(0) = \mathbf{b}_0 \dot{\mathbf{V}} & \dot{I}(0) = \mathbf{b}_0 \dot{\mathbf{I}} \\ \dot{V}(L) = \mathbf{b}_L \dot{\mathbf{V}} & \dot{I}(L) = \mathbf{b}_L \dot{\mathbf{I}} \end{cases} \quad (13)$$

where \mathbf{b}_0 and \mathbf{b}_L are vectors of constant elements being the values of the function of the wavelet basis respectively at the left border and at the right border of the space interval.

Equations (12) can be rewritten as

$$\begin{cases} \mathbf{b}_0 \dot{\mathbf{V}} + Z_s \mathbf{b}_0 \dot{\mathbf{I}} = \dot{E} \\ \mathbf{b}_L \dot{\mathbf{V}} = Z_L \mathbf{b}_L \dot{\mathbf{I}} \end{cases} \quad (14)$$

Taking into account the equations (11) and (14) we can write the following system as shown in (4):

$$\begin{cases} (\mathbf{D}_z + \mathbf{B}_0)\dot{\mathbf{V}} + (Z_2(\omega)\mathbf{Z}_1 + Z_s\mathbf{B}_0)\dot{\mathbf{I}} = \dot{\mathbf{E}} \\ (Y_2(\omega)\mathbf{Y}_1 + \mathbf{B}_0)\dot{\mathbf{V}} + (\mathbf{D}_z - Z_L\mathbf{B}_L)\dot{\mathbf{I}} = 0 \end{cases} \quad (15)$$

where \mathbf{B}_0 and \mathbf{B}_L are matrices with all rows equal respectively to \mathbf{b}_0 and \mathbf{b}_L .

The way the boundary conditions are imposed here is due to the fact that the matrices \mathbf{B}_0 and \mathbf{B}_L are highly sparse (since only N entries of the vectors \mathbf{b}_0 and \mathbf{b}_L are different from zero), besides this method doesn't require any further calculation or additional equations to add to the system.

Equations (15) can be rewritten in the following form

$$\begin{vmatrix} \mathbf{D}_z + \mathbf{B}_0 & Z_2(\omega)\mathbf{Z}_1 + Z_s\mathbf{B}_0 \\ Y_2(\omega)\mathbf{Y}_1 + \mathbf{B}_0 & \mathbf{D}_z - Z_L\mathbf{B}_L \end{vmatrix} \begin{vmatrix} \dot{\mathbf{V}} \\ \dot{\mathbf{I}} \end{vmatrix} = \begin{vmatrix} \dot{\mathbf{E}} \\ 0 \end{vmatrix} \quad (16)$$

System (16) is a square system of dimension $2n \times 2n$; its solutions gives the behavior of the unknowns along the line (function of z) in the wavelet domain for each frequency. The standard inverse FFT is used to obtain the time domain response.

3.2 Integral formulation

In order to include the boundary conditions we integrate (7) respectively between 0 and z , and between z and L obtaining the two following systems

$$\begin{cases} \dot{V}(z) - \dot{V}(0) = -Z_2(\omega) \int_0^z Z_1(z) \dot{I}(z) dz \\ \dot{I}(z) - \dot{I}(0) = -Y_2(\omega) \int_0^z Y_1(z) \dot{V}(z) dz \end{cases} \quad (17)$$

and

$$\begin{cases} \dot{V}(L) - \dot{V}(z) = -Z_2(\omega) \int_z^L Z_1(z) \dot{I}(z) dz \\ \dot{I}(L) - \dot{I}(z) = -Y_2(\omega) \int_z^L Y_1(z) \dot{V}(z) dz \end{cases} \quad (18)$$

Substituting the expansion (9) into (17) and (18) we obtain

$$\begin{cases} \mathbf{b}(z)\dot{\mathbf{V}} - \mathbf{b}(z)\dot{\mathbf{V}}_0 = -Z_2(\omega) \int_0^z \mathbf{b}(z)\mathbf{Z}_1\dot{\mathbf{I}} dz \\ \mathbf{b}(z)\dot{\mathbf{I}} - \mathbf{b}(z)\dot{\mathbf{I}}_0 = -Y_2(\omega) \int_0^z \mathbf{b}(z)\mathbf{Y}_1\dot{\mathbf{V}} dz \end{cases} \quad (19)$$

and

$$\begin{cases} \mathbf{b}(z)\dot{\mathbf{V}}_L - \mathbf{b}(z)\dot{\mathbf{V}} = -Z_2(\omega) \int_z^L \mathbf{b}(z)\mathbf{Z}_1\dot{\mathbf{I}} dz \\ \mathbf{b}(z)\dot{\mathbf{I}}_L - \mathbf{b}(z)\dot{\mathbf{I}} = -Y_2(\omega) \int_z^L \mathbf{b}(z)\mathbf{Y}_1\dot{\mathbf{V}} dz \end{cases} \quad (20)$$

where the quantities $\dot{\mathbf{V}}_0$, $\dot{\mathbf{V}}_L$, $\dot{\mathbf{I}}_0$ and $\dot{\mathbf{I}}_L$ are the wavelet transform of $\dot{V}(0)$, $\dot{V}(L)$, $\dot{I}(0)$, $\dot{I}(L)$.

Taking into account the definition of the integral operator we obtain for equations (17) and (18)

$$\begin{cases} \dot{\mathbf{V}} - \dot{\mathbf{V}}_0 = -Z_2(\omega)\mathbf{T}_z\mathbf{Z}_1\dot{\mathbf{I}} \\ \dot{\mathbf{I}} - \dot{\mathbf{I}}_0 = -Y_2(\omega)\mathbf{T}_z\mathbf{Y}_1\dot{\mathbf{V}} \end{cases} \quad (21)$$

$$\begin{cases} \dot{\mathbf{V}}_L - \dot{\mathbf{V}} = -Z_2(\omega)\mathbf{T}_z^T\mathbf{Z}_1\dot{\mathbf{I}} \\ \dot{\mathbf{I}}_L - \dot{\mathbf{I}} = -Y_2(\omega)\mathbf{T}_z^T\mathbf{Y}_1\dot{\mathbf{V}} \end{cases} \quad (22)$$

In (21) and (22) \mathbf{T}_z is the integral operator, which is transposed in (22) because the integration is from z to L .

The boundary conditions (12) can be also rewritten in the wavelet domain in the following form:

$$\begin{cases} \dot{\mathbf{V}}_0 + Z_s\dot{\mathbf{I}}_0 = \dot{\mathbf{E}} \\ \dot{\mathbf{V}}_L = Z_L\dot{\mathbf{I}}_L \end{cases} \quad (23)$$

By multiplying the second equation of (21) by Z_s and the second equation of (22) by Z_L , adding them and considering the boundary conditions (23) we obtain the following system:

$$\begin{cases} \dot{\mathbf{V}} + Z_s \dot{\mathbf{I}} + Z_2(\omega) \mathbf{T}_z \mathbf{Z}_1 \dot{\mathbf{I}} + Z_s Y_2(\omega) \mathbf{T}_z \mathbf{Y}_1 \dot{\mathbf{V}} = \dot{\mathbf{E}} \\ -\dot{\mathbf{V}} + Z_L \dot{\mathbf{I}} + Z_2(\omega) \mathbf{T}_z^T \mathbf{Z}_1 \dot{\mathbf{I}} - Z_L Y_2(\omega) \mathbf{T}_z^T \mathbf{Y}_1 \dot{\mathbf{V}} = 0 \end{cases} \quad (24)$$

which can be written in a matrix form:

$$\begin{vmatrix} \mathbf{I}_d + Z_s Y_2(\omega) \mathbf{T}_z \mathbf{Y}_1 & Z_2(\omega) \mathbf{T}_z \mathbf{Z}_1 + Z_s \mathbf{I}_d \\ -\mathbf{I}_d - Z_L Y_2(\omega) \mathbf{T}_z^T \mathbf{Y}_1 & Z_2(\omega) \mathbf{T}_z^T \mathbf{Z}_1 + Z_L \mathbf{I}_d \end{vmatrix} \begin{vmatrix} \dot{\mathbf{V}} \\ \dot{\mathbf{I}} \end{vmatrix} = \begin{vmatrix} \dot{\mathbf{E}} \\ 0 \end{vmatrix} \quad (25)$$

where \mathbf{I}_d is the identity matrix of proper dimension. System (25) is a square system and the solution is obtained directly. This comes from the fact that the boundary conditions are already included in the integral equations.

3.3 Generalization for a multiconductor line

In case the line is multiconductor (constituted by $n+1$ conductors) $\dot{\mathbf{V}}$ and $\dot{\mathbf{I}}$ in (7) are vectors composed by the single conductor quantities $\dot{V}_1, \dots, \dot{V}_p$ and $\dot{I}_1, \dots, \dot{I}_p$; while the line parameters $Z(z, \omega)$ and $Y(z, \omega)$ are matrices. Operating as in the previous paragraph, for both the differential and the integral formulation, we obtain again a system in the form of (16) or (25) with the following differences from the single conductor case:

$$\dot{\mathbf{V}} = \begin{vmatrix} \dot{V}_1 \\ \dot{V}_2 \\ \vdots \\ \dot{V}_p \end{vmatrix} \quad \dot{\mathbf{I}} = \begin{vmatrix} \dot{I}_1 \\ \dot{I}_2 \\ \vdots \\ \dot{I}_p \end{vmatrix}$$

where \dot{V}_i and \dot{I}_i are vectors of dimension n .

The operator matrices \mathbf{D}_z and \mathbf{T}_z become (only \mathbf{D}_z is shown)

$$\bar{\mathbf{D}}_z = \begin{vmatrix} \mathbf{D}_z & 0 & 0 & \cdots & 0 \\ 0 & \mathbf{D}_z & 0 & \cdots & 0 \\ \vdots & \vdots & \vdots & \ddots & \vdots \\ 0 & 0 & 0 & \cdots & \mathbf{D}_z \end{vmatrix}$$

and the matrix \mathbf{B}_0 becomes

$$\bar{\mathbf{B}}_0 = \begin{vmatrix} \mathbf{B}_0 & 0 & 0 & \cdots & 0 \\ 0 & \mathbf{B}_0 & 0 & \cdots & 0 \\ \vdots & \vdots & \vdots & \ddots & \vdots \\ 0 & 0 & 0 & \cdots & \mathbf{B}_0 \end{vmatrix}$$

The matrices of the parameters in the wavelet domain become

$$Z_2(\omega) \mathbf{Z}_1 = \begin{vmatrix} (Z_2(\omega) \mathbf{Z}_1)_{11} & (Z_2(\omega) \mathbf{Z}_1)_{12} & \cdots & (Z_2(\omega) \mathbf{Z}_1)_{1p} \\ (Z_2(\omega) \mathbf{Z}_1)_{21} & (Z_2(\omega) \mathbf{Z}_1)_{22} & \cdots & (Z_2(\omega) \mathbf{Z}_1)_{2p} \\ \vdots & \vdots & \ddots & \vdots \\ (Z_2(\omega) \mathbf{Z}_1)_{p1} & (Z_2(\omega) \mathbf{Z}_1)_{p2} & \cdots & (Z_2(\omega) \mathbf{Z}_1)_{pp} \end{vmatrix}$$

where $(Z_2(\omega) \mathbf{Z}_1)_{i,j}$ are matrices related to each value of the matrix of the impedance. As for the impedances Z_L and Z_s , they become matrices as follows

$$\mathbf{Z}_L = \begin{vmatrix} Z_{L11} \mathbf{I}_d & Z_{L12} \mathbf{I}_d & \cdots & Z_{L1p} \mathbf{I}_d \\ Z_{L21} \mathbf{I}_d & Z_{L22} \mathbf{I}_d & \cdots & Z_{L2p} \mathbf{I}_d \\ \vdots & \vdots & \ddots & \vdots \\ Z_{Lp1} \mathbf{I}_d & Z_{Lp2} \mathbf{I}_d & \cdots & Z_{Lpp} \mathbf{I}_d \end{vmatrix}$$

where \mathbf{I}_d is the identity matrix of dimension $n \times n$ and the single impedances Z_{Lij} are determined, for instance, by a nodal analysis at the ports of the Multiconductor Line. As for the input voltages the resulting known term is

$$\dot{\mathbf{E}} = \begin{bmatrix} \dot{\mathbf{E}}_1 \\ \dot{\mathbf{E}}_2 \\ \vdots \\ \dot{\mathbf{E}}_p \end{bmatrix}$$

4 Numerical results

The proposed methods have been first validated on a single conductor lossless line closed on its characteristic resistance, then tested on several cases, both with and without frequency dependent parameters, and compared with a standard FD method. Some results are reported here.

As for the CPU times the systems can be solved by standard methods or by methods optimized for sparse matrices. In the latter case, performed here in this paper, in order to obtain high sparsity and good numerical properties the matrices need to be divided into their real and imaginary part, and the systems need to be solved separately. This is because of the large difference in the magnitudes of the real and imaginary parts. With this procedure we are able to obtain CPU times that are proportional to the dimension of the matrix, instead of to the square of it. The integral and the differential approaches proposed here give the same results, in all the simulation we have performed, hence only one of the two methods are reported in the results.

4.1 Validation of the methods

In order to verify the validity of the methods, they have been tested on a single conductor lossless line with no input resistance and terminated on its characteristic impedance. Its parameters are respectively

$$l = 28\mu H/m \quad c = 1.2nF/m$$

hence the characteristic impedance is $R_0 = 152.7525\Omega$; the line length is $0.03m$.

Figure 1 shows the input and output voltage of the line calculated both by the method proposed here and a standard FD code. It is clearly visible that the signal is transmitted to the end of the line without reflections and with no attenuation. The transit time is also respected. The comparison has been made in

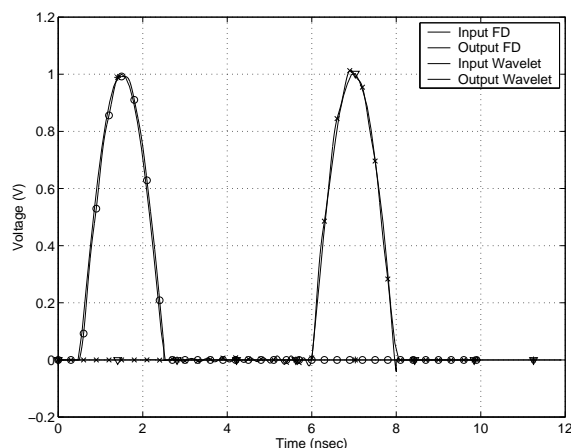


Figure 1: Input and output voltages of the lossless line

this case since an analytical solution is available, and the results have been compared given the same number

of samples in the frequency domain. In order to obtain results with the same accuracy a CPU time of one order of magnitude greater is necessary with a FD code. The main reason is that in order to obtain results with the same accuracy a greater number of spatial unknowns (around one order of magnitude) must be chosen. This fact shows the good interpolating properties of the wavelet basis.

4.2 Single conductor line

The nonuniform conductor line considered here is represented in figure 2 and it is characterized by the following parameters:

$$c(x) = \begin{cases} 1.621 & 0 \leq x \leq 1 \\ 2.413 - 0.792x & 1 \leq x \leq 2 \\ 0.829 & 2 \leq x \leq 3 \end{cases} \text{ pF/cm}$$

$$l(x) = \begin{cases} 2.09 & 0 \leq x \leq 1 \\ 0.545 + 2.763x - 1.838x^2 + 0.6168x^3 & 1 \leq x \leq 2 \\ 3.657 & 2 \leq x \leq 3 \end{cases} \text{ nH/cm}$$

$$r_{dc}(x) = \begin{cases} 4.0 & 0 \leq x \leq 1 \\ 2.4/(1 - 0.4x) & 1 \leq x \leq 2 \\ 12.0 & 2 \leq x \leq 3 \end{cases} \Omega/cm$$

$$g(x) = 0S/m$$

$$R_1 = R_2 = 10\Omega; \quad L = 3cm$$

The variation of r with the frequency is given by

$$r(x, \omega) = r_{dc}(x) + kr_{dc}(x)\sqrt{2j\omega} \quad (26)$$

where $k = 0.417 \times 10^{-5}$

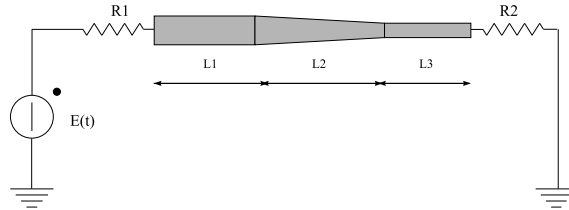


Figure 2: Single conductor nonuniform line

The input signal is an exponential function whose expression is $E(t) = 1e^{-10t}$.

Figures 3 show the input and output voltages of the line respectively with $k = 0.417 \times 10^{-5}$ and $k = 0$ (no frequency dependence). The results have been obtained with a number of wavelets equal to 256 and a CPU time of 12 minutes.

Comparing the two figures it can be noted the smoothing effect of the frequency dependence.

Figures 4 show the same results previously obtained but with a number of wavelet equal to 64 and a CPU time of 3 minutes. It can be noted that even with very few wavelet coefficients the results are clearly acceptable; furthermore the results remain stable as the number of wavelet coefficient increases. These are general trends observed in the considered tests.

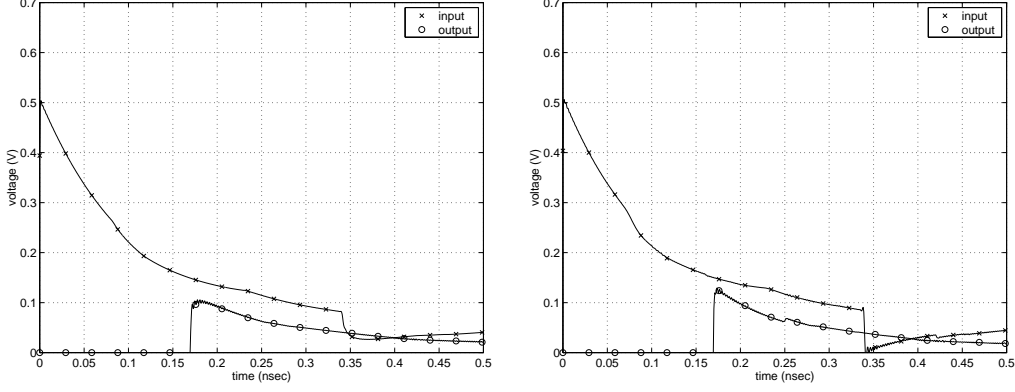


Figure 3: Input and output voltages with and without frequency dependence (n=256)

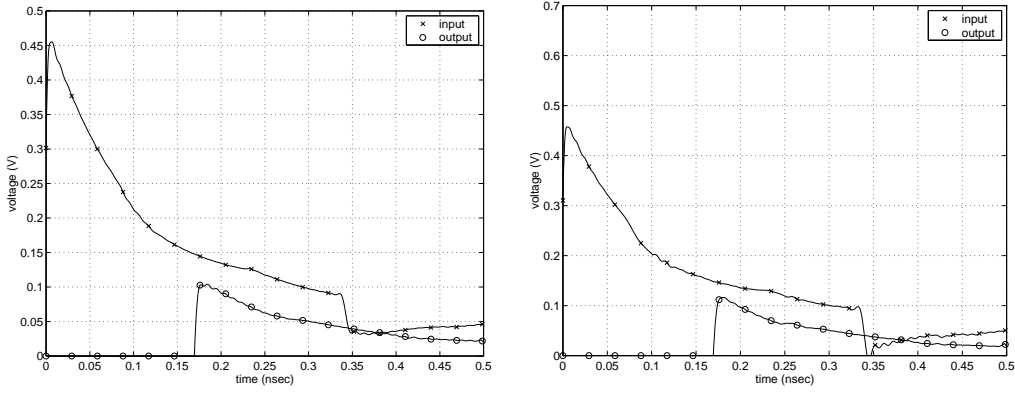


Figure 4: Input and output voltages with and without frequency dependence (n=64)

4.3 Multiconductor line

The behavior of a frequency dependent two conductor line has been investigated, both with a resistive load and a capacitive load.

4.3.1 Resistive load

The nonuniform two conductor line considered here is represented in figure 5 and it is characterized by the following parameters:

$$c(x) = \begin{vmatrix} 122 & -50 \\ -50 & 122 \end{vmatrix} \left(1 + \frac{x}{L}\right)^{-2} pF/m$$

$$l(x) = \begin{vmatrix} 280 & 70 \\ 70 & 280 \end{vmatrix} \left(1 + \frac{x}{L}\right)^2 nH/m$$

$$g(x) = \begin{vmatrix} 2.3 & 0 \\ 0 & 2.3 \end{vmatrix} \left(1 + \frac{x}{L}\right)^{-2} \mu S/m$$

$$r_{dc}(x) = \begin{vmatrix} 0.2 & 0 \\ 0 & 0.2 \end{vmatrix} \left(1 + \frac{x}{L}\right)^2 \Omega/m$$

$$R_1 = R_2 = 10\Omega \quad R_3 = R_4 = 50\Omega$$

The line length is $L = 3cm$ and the input signal is a half sine between time $t = 0.2nsec$ and $t = 0.4nsec$. The variation of r with the frequency is given by:

$$r(x, f) = r_{dc}(x)(1 + k\sqrt{f}) \quad (27)$$

where $k = 0.1$.



Figure 5: Double conductor nonuniform line

Figures 6 show the input and output voltages at the ends of the line in case of frequency dependence:

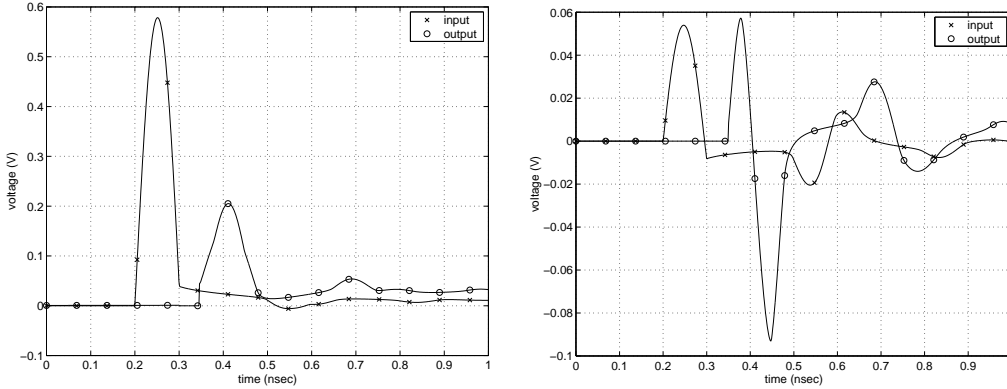


Figure 6: Input and output voltages of both conductor with frequency dependence

Figures 7 show the input and output voltages at the ends of the line in case of no frequency dependence:

In the two conductor line the results have been obtained with a number of wavelets equal to 128. The comparison between the figures shows again the smoothing effect of the frequency dependence.

4.3.2 Capacitive load

The nonuniform two conductor line considered here is represented in figure 8 and the capacitive load (parallel between a resistor and a capacitor) is the representation of the nominal value of the input impedance of a CMOS inverter corresponding to $1\mu m$ gate technology.

The line parameters are the same as before, with

$$R_4 = 1M\Omega, \quad C = 0.1pF$$

and the input and output voltages at both the conductors are investigated.

Figures 9 show the input and output voltages at the ends of the line in case of frequency dependence.

Figures 10 show the input and output voltages at the ends of the line in case of no frequency dependence:

The results show that the capacitive load enhances the signal transmission when the CMOS is energized, with respect to the results obtained in absence of capacitance. On the other hand the frequency dependence of the parameters has the same effect of reducing the amplitude of the transmitted signals.

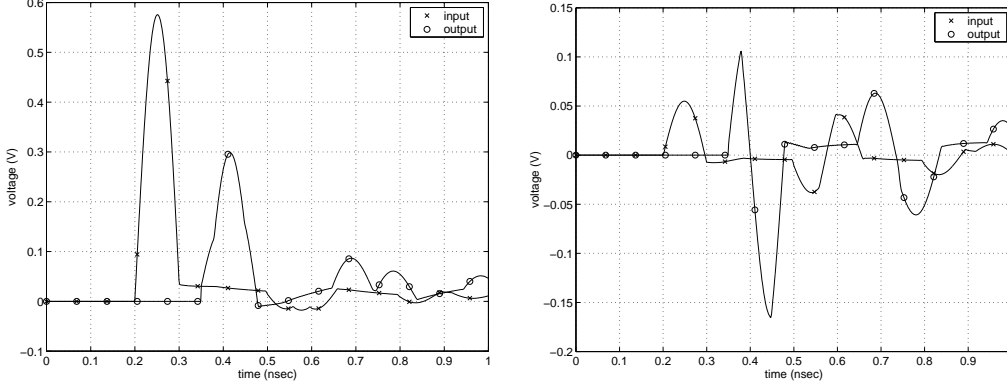


Figure 7: Input and output voltages of both conductors with no frequency dependence



Figure 8: Double conductor nonuniform line with capacitive load

Other tests have been performed on a uniform line having the same configuration of figure 8, characterized by the parameters:

$$c = \begin{vmatrix} 122 & -50 \\ -50 & 122 \end{vmatrix} pF/m \quad l = \begin{vmatrix} 280 & 70 \\ 70 & 280 \end{vmatrix} nH/m$$

$$g = \begin{vmatrix} 2.3 & 0 \\ 0 & 2.3 \end{vmatrix} \mu S/m \quad r_{dc} = \begin{vmatrix} 0.2 & 0 \\ 0 & 0.2 \end{vmatrix} \Omega/m$$

$$R_1 = R_2 = 10\Omega \quad R_3 = 50\Omega$$

$$R_4 = 1M\Omega, \quad C = 0.1pF$$

$$r(f) = r_{dc}(1 + k\sqrt{f}) \quad (28)$$

where $k = 0.1$. The line length is again $L = 3cm$ and the input signal is the same as before.

Figures 11 show the input and output voltages at the ends of the line in case of frequency dependence:

Figures 12 show the input and output voltages at the ends of the line in case of no frequency dependence:

Comparing this last two figures (11 and 12) with (9 and 10) it can be seen that the effect of the frequency dependence is qualitatively the same one (signal smoothing and reduction) but it is more evident in a nonuniform line than in a uniform line. This trend is also shown in [6].

5 Conclusions

The method proposed here for the analysis of high speed interconnects with frequency dependent parameters is based on wavelet expansion in the space domain and FFT in the frequency domain. The tests performed on many cases have demonstrated that the method is efficient and reliable also with low memory and low CPU time requirements.

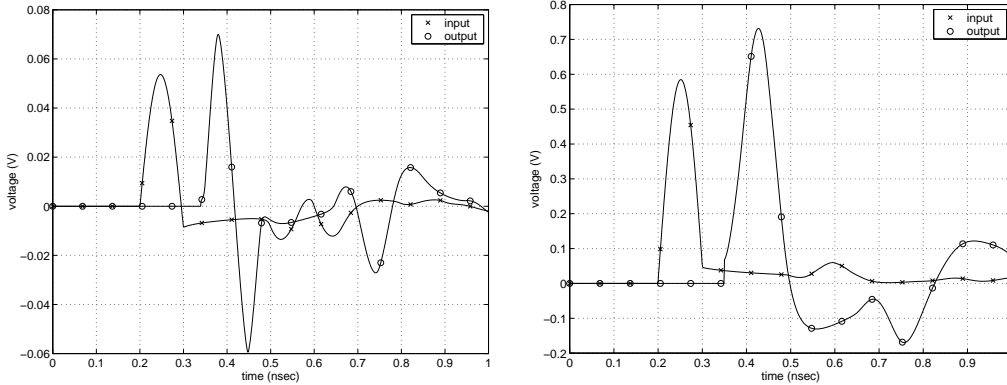


Figure 9: Input and output voltages of both conductors with frequency dependence

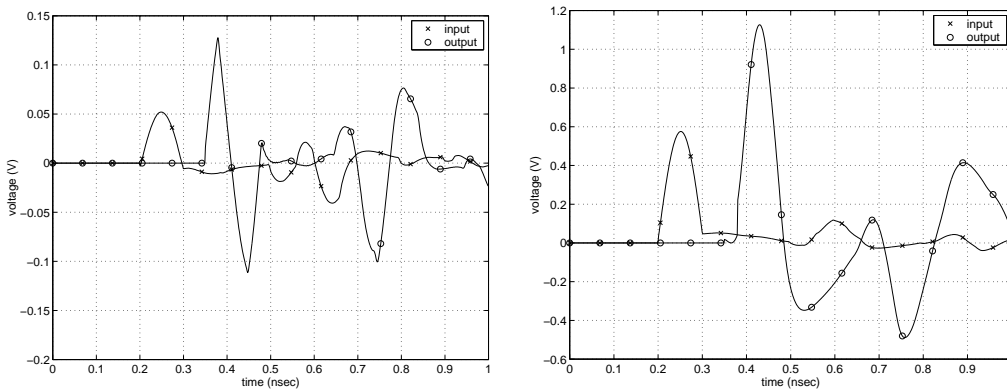


Figure 10: Input and output voltages of both conductors with no frequency dependence

References

- [1] A. Djordjevic, T. Sarkar, "Analysis of time response of lossy multiconductor transmission line network" *IEEE Trans. MTT Vol 35, n. 10, Oct. 1987, pp 898-907.*
- [2] J. E. Shutt-Aine, "Transient analysis of nonuniform transmission lines" *IEEE Trans. CAS-1 Vol. 39 n. 5, May. 1992, pp 378-385.*
- [3] F. Y. Chang, "Transient simulation of nonuniform coupled lossy transmission lines characterized with frequency dependent parameters - part I: waveform relaxation analysis" *IEEE Trans. CAS-39, n. 8, August 1992, pp 585-603.*
- [4] E. C. Chang, S. M. Kang, "Computationally efficient simulation of a lossy transmission line with skin effect by using numerical inversion of laplace transform" *IEEE Trans. On CAS-1. Vol. 39, n. 11, Nov. 1992, pp 861-868.*
- [5] H. Heeb, A. E. Ruehli, "Three-dimensional interconnect analysis using partial element equivalent circuits" *IEEE Trans. On CAS-1. Vol. 39, n. 11, Nov. 1992, pp 974-982.*
- [6] V. K. Tripathi, N. Orhanovic, "Time - domain characterization and analysis of dispersive dissipative interconnects" *IEEE Trans. On CAS-1. Vol. 39, n. 11, Nov. 1992, pp 938-945.*
- [7] T. Dhaene, L. Martens, D. De Zutter, "Transient simulation of arbitrary nonuniform interconnection structures characterized by scattering parameters" *IEEE Trans. On CAS-1. Vol. 39, n. 11, Nov. 1992, pp 928-937.*

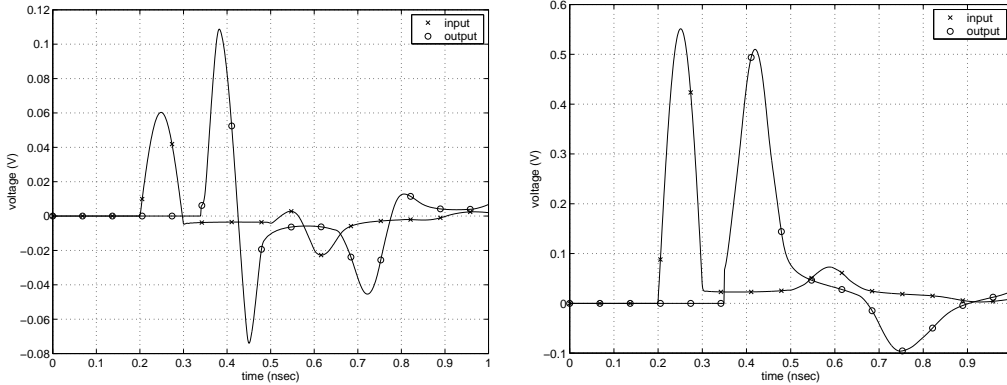


Figure 11: Input and output voltages of both conductors with frequency dependence

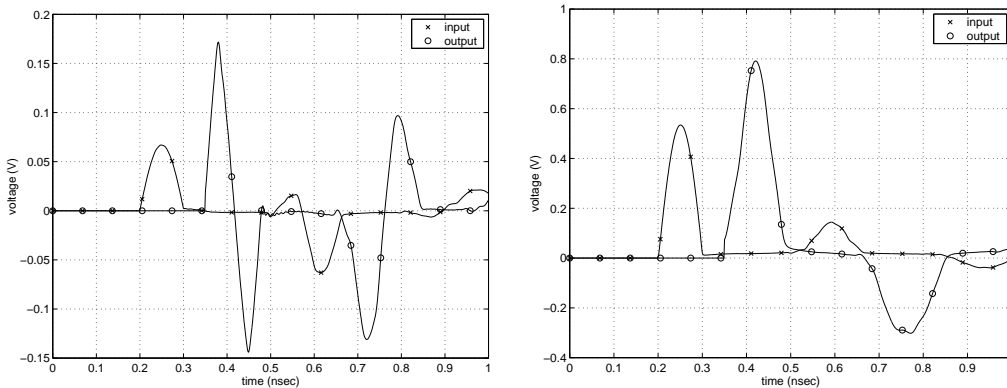


Figure 12: Input and output voltages of conductor 1 with no frequency dependence

- [8] F. Y. Chang, "Transient simulation of frequency - dependent nonuniform coupled lossy transmission lines" *IEEE Trans. On CPM Tech.- B. Vol. 17, n. 1, Feb. 1994, pp 3-14.*
- [9] L. Corti, G. Miano, L. Verolino "A new technique for simulating nonlinear loaded lossy lines" *IEEE Trans. MAG Vol. 32, n. 3, May 1996, pp 934-937.*
- [10] A. Orlandi, C. R. Paul, "FDTD analysis of lossy, multiconductor transmission lines terminated in arbitrary loads" *IEEE Trans. On EMC. Vol. 38, n. 3, Aug. 1996, pp 388-398.*
- [11] S. Grivet-Talocia, F. Canavero, "Wavelet-based adaptive solution for the nonuniform multiconductor transmission lines" *IEEE Microwave and Guided Wave Letters, vol.8, pp.287-289, August 1998.*
- [12] S. Barmada, M. Raugi, "Transient Numerical Solutions of nonuniform MTL equations with Nonlinear Loads by Wavelet Expansion in Time or Space Domain" " *IEEE Transactions on Circuits and Systems August 2000, Vol 47, n 8, pp-1178 - 1190*
- [13] S. Barmada, M. Raugi, "Space - time wavelet expansion iterative solution of nonuniform transmission lines with arbitrary loads" *International Journal of Numerical Modelling, Vol 28, n 3, 2001, pp 219-235*
- [14] C. K. Chui, "Wavelets: a tutorial in theory and applications" *New York, Academic Press, 1992.*
- [15] A.Cohen, I. Daubechies, B. Jawerth, P. Vial, "Multiresolution analysis wavelets and fast algorithms on the interval" *C. R. Acad. Sci. Paris ser. i Math. Vol 316, 1992, pp 417-421.*

- [16] T. K. Sarkar, C. Su, R. Adve, M. Salazar-Palma, L. Garcia-Castillo, R. R. Boix, "A tutorial on wavelets from an electrical engineering perspective, Part 1: Discrete Wavelet Techniques" *IEEE Antennas and Propagation Magazine*, Vol. 40, No 5, October 1998.
- [17] G. Beylkin "Wavelets and fast numerical algorithms" *Proc. of Symposia in Applied Math. Vol 47, 1993*
- [18] R. L. Wiginton, N. S. Nahman "Transient analysis of coaxial cables considering skin effect" *Proc IRE*, pp.166 - 174, Feb. 1957
- [19] N. S. Nahman, D. R. Holt "Transient analysis of coaxial cables using the skin effect approximation $A + B\sqrt{s}$ " *IEEE Trans Circuit Theory*, vol CT - 19. pp. 443 -451, Sept. 1972